Transmission of electromagnetic waves through thin metal films with randomly rough surfaces

J. A. Sánchez-Gil* and A. A. Maradudin
Department of Physics and Institute for Surface and Interface Science, University of California, Irvine, California 92717

Jun Q. Lu
Surface Optics Corporation, P.O. Box 261602, San Diego, California 92126

V. D. Freilikher
The Jack and Pearl Resnick Institute of Advanced Technology, Department of Physics, Bar-Ilan University, Ramat-Gan 52900, Israel
(Received 6 September 1994)

By means of perturbation theory and a computer simulation approach we study the transmission of p-polarized electromagnetic waves through a thin, free-standing metal film. The illuminated (upper) surface is a one-dimensional, randomly rough surface: the back surface is planar. The plane of incidence is perpendicular to the generators of the rough surface. The film is sufficiently thin that the two surface plasmon polaritons it supports in the absence of the roughness have distinct wave numbers $q_1(\omega)$ and $q_2(\omega)$ at the frequency ω of the incident wave. As a consequence, the angular dependence of the intensity of the incoherent component of the transmitted field displays satellite peaks at angles of transmission θ_t that are related to the angle of incidence θ_0 by $\sin\theta_t=-\sin\theta_0\pm(c/\omega)[q_2(\omega)-q_1(\omega)]$, in addition to the enhanced transmission peak. Analogous satellite peaks are also present in the angular dependence of the intensity of the incoherent component of the reflected field, in addition to the enhanced backscattering peak.

I. INTRODUCTION

In a recent paper by McGurn and one of the present authors,[1] the transmission of light through a thin, free-standing, metal film, whose illuminated face was a one-dimensional, randomly rough surface, while the back surface was perfectly planar, was studied by means of infinite-order perturbation theory. It was assumed that the mean thickness of the film was sufficiently thin that an observable fraction of the incident light was transmitted through it. At the same time the simplifying assumption was made that it was thick enough that the two surface plasmon polaritons supported by the film in the absence of the roughness were degenerate. The principal result of this study was that the transmitted light displayed the phenomenon of enhanced transmission, viz., a well-defined peak in the angular dependence of the intensity of the incoherent component of the transmitted light in the antispecular direction.

The existence of enhanced transmission was subsequently confirmed by the results of computer simulation studies of the transmission of light through such metal films.[2] It was also observed experimentally.[2-4]

However, the assumption that the mean thickness of the film was large enough that the surface plasmon polaritons supported by it could be regarded as degenerate had the consequence that another interesting consequence of the multiple scattering of the surface plasmon polaritons excited by the incident electromagnetic waves through the random surface roughness was not obtained. This is the presence of a satellite peak on each side of the enhanced transmission peak. In this paper, by both a perturbation-theoretic calculation and computer simulation studies we demonstrate the existence of these satellite peaks.

To understand the physical origin of the enhancement of transmission into directions other than the antispecular direction, let us first consider a scattering system that is more general than the metal film to which this paper is devoted. Thus we consider the scattering of electromagnetic waves from, and their transmission through, a semi-infinite random medium. In the case of scattering, to each multiple-scattering path $ABCD$ [Fig. 1(a)] there always corresponds a time-reversed partner $A'CBD'$, in which the wave strikes the same scatterers, but in the reverse order. The phase difference between these two paths is

$$\Delta\phi=\mathbf{r}_{BC}\cdot(\mathbf{k}_{\rm in}+\mathbf{k}_{\rm sc}) , \tag{1.1}$$

where $\mathbf{k}_{\rm in}$ and $\mathbf{k}_{\rm sc}$ are the wave vectors of the incident and scattered field, respectively, while $\mathbf{r}_{BC}$ is the vector joining the scatterers B and C. Constructive interference ($\Delta\phi=0$) occurs when $\mathbf{k}_{\rm sc}=-\mathbf{k}_{\rm in}$, or equivalently when

$$k_{{\rm sc},\parallel}=-k_{{\rm in},\parallel} \quad\text{and}\quad k_{{\rm sc},\perp}=-k_{{\rm in},\perp} , \tag{1.2}$$

where $k_{{\rm in},\parallel}$ and $k_{{\rm in},\perp}$ are the components of $\mathbf{k}_{\rm in}$ parallel and perpendicular to the mean interface, respectively, while $k_{{\rm sc},\parallel}$, and $k_{{\rm sc},\perp}$ are the corresponding components of $\mathbf{k}_{\rm sc}$. The conditions (1.2) describe scattering into the retroreflection direction, and this gives rise to enhanced backscattering.

In transmission, we reflect the scattered wave in the mean scattering surface ($\hat{x}_3\rightarrow-\hat{x}_3$ where $\hat{x}_3$ is the unit vector normal to the mean interface). The phase difference between the multiple-scattering path $ABCE$ and its time-reversed partner $A'CBE'$ [Fig. 1(a)] is then

$$\Delta\phi = \mathbf{r}_{BC}\cdot(\mathbf{k}_{\text{in}}+\mathbf{k}_{\text{sc}}^{*}) \;, \tag{1.3a}$$

where the vector $\mathbf{k}_{\text{sc}}^{*}$ is defined by

$$\mathbf{k}_{\text{sc}}^{*} = k_{\text{sc}\parallel}^{*}\hat{x}_1 + k_{\text{sc},\perp}(-\hat{x}_3) \;. \tag{1.3b}$$

In this case coherent interference ($\Delta\phi=0$) now occurs when $\mathbf{k}_{\text{sc}}^{*}=-\mathbf{k}_{\text{in}}$, i.e., when

$$k_{\text{sc},\parallel} = -k_{\text{in},\parallel} \quad\text{and}\quad k_{\text{sc},\perp} = k_{\text{in},\perp} \;. \tag{1.4}$$

The conditions (1.4) described scattering (transmission) into the antispecular direction, and this gives rise to enhanced transmission.

Let us turn now to the case in which the scattering system is a bounded random medium that supports N guided waves, whose wave numbers at the frequency of the incident electromagnetic wave ω are $k_1(\omega), k_2(\omega), \ldots, k_N(\omega)$. In the case of scattering each trajectory $ABCD$ is now N-fold degenerate in the sense that along the segment BC there are N "channels" with different phase factors. The phase difference between the multiple-scattering path $(ABCD)_m$ and its time-reversed partner $(A'CBD')_n$ [Fig. 1(b)] is[5]

$$\Delta\phi_{nm} = \mathbf{r}_{BC}\cdot(\mathbf{k}_{\text{in}}+\mathbf{k}_{\text{sc}}) + |\mathbf{r}_{BC}|(k_n-k_m) \;. \tag{1.5}$$

We see from Eq. (1.5) that constructive interference ($\Delta\phi_{nm}=0$) can now occur not only for scattering into the retroreflection direction ($n=m$, $\mathbf{k}_{\text{sc}}=-\mathbf{k}_{\text{in}}$), which is the case for infinite and semi-infinite media where $k_n=k_m=k$, but also for scattering into other directions $\mathbf{k}_{\text{sc}}\neq-\mathbf{k}_{\text{in}}$ for which $\Delta\phi_{nm}=0$ for some $n\neq m$.

The situation is similar in the case of transmission. The phase difference between the path $(ABCE)_m$ and its time-reversed partner $(A'CBE')_n$ [Fig. 1(b)] is

$$\Delta\phi_{nm} = \mathbf{r}_{BC}\cdot(\mathbf{k}_{\text{in}}+\mathbf{k}_{\text{sc}}^{*}) + |\mathbf{r}_{BC}|(k_n-k_m) \;. \tag{1.6}$$

In this case constructive interference ($\Delta\phi_{nm}=0$) now occurs not only for scattering into the antispecular direction ($n=m$, $\mathbf{k}_{\text{sc}}^{*}=-\mathbf{k}_{\text{in}}$), but also for scattering into other directions $\mathbf{k}_{\text{sc}}^{*}\neq-\mathbf{k}_{\text{in}}$ for which $\Delta\phi_{nm}=0$ for some $n\neq m$.

Thus, on the basis of the preceding arguments, in the scattering of electromagnetic waves from bounded structures that support two or more guided waves at the frequency ω of the scattered wave we expect to see satellite peaks in addition to the enhanced backscattering peak and the enhanced transmission peak in reflection and transmission, respectively.

The system to be studied in this paper, a thin metal film, supports two and only two surface plasmon polaritons at a given frequency for any thickness of the film, although their wave numbers approach one another as the thickness of the film becomes very large. If we denote the wave numbers of these two surface plasmon polaritons at the frequency ω by $q_1(\omega)$ and $q_2(\omega)$, then the argument just given predicts that the two satellite peaks occur at transmission angles θ_t given by

$$\sin\theta_t = -\sin\theta_0 \pm \frac{c}{\omega}[q_1(\omega)-q_2(\omega)] \;, \tag{1.7}$$

where θ_0 is the angle of incidence. It is our intention to verify this result.

In so doing we will also show that the enhanced backscattering peak that is known to be present in the angular dependence of the intensity of the electromagnetic waves scattered incoherently from a metal film whose illuminated surface is randomly rough while its back surface is planar,[1,2] will also acquire two satellite peaks, at scattering angles θ_s given by

$$\sin\theta_s = -\sin\theta_0 \pm \frac{c}{\omega}[q_1(\omega)-q_2(\omega)] \;, \tag{1.8}$$

a result that follows from Eq. (1.5).

The outline of this paper is the following. In Sec. II we describe the free-standing metal film with a one-dimensional, randomly rough surface whose scattering and transmission properties will be studied in this work. In Sec. III we derive the dispersion relations for the two

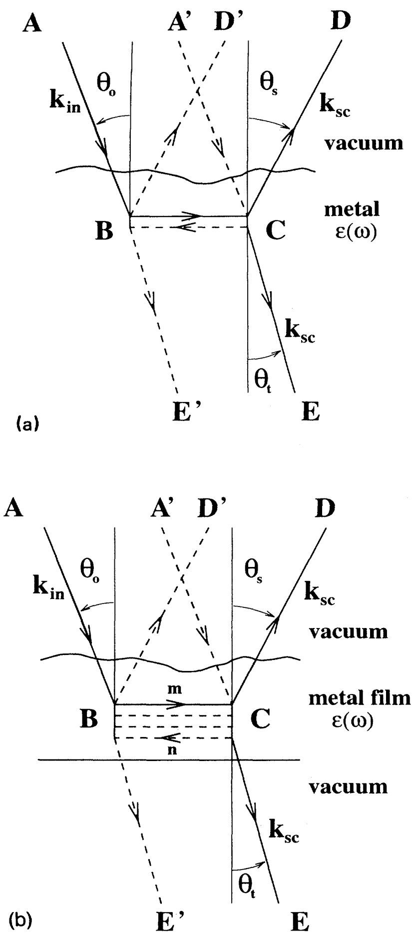

FIG. 1. (a) Multiple-scattering sequences occurring in the scattering of electromagnetic waves from, and their transmission into, a semi-infinite random medium, and their time-reversed partners; (b) multiple-scattering sequences occurring in the scattering of electromagnetic waves from, and their transmission through, a bounded structure that supports several guided waves, and their time-reversed partners.

surface plasmon polaritons supported by such a film in the absence of the roughness, and discuss the properties of their solutions that will be needed in the calculations that follow. The angular dependence of the intensity of the incoherent component of p-polarized electromagnetic waves scattered from and transmitted through the rough film will be calculated perturbatively in Sec. IV, exactly through terms of fourth order in the surface profile function. The same calculations will be carried out nonperturbatively in Sec. V, by a computer simulation approach for a film with a rougher surface than can be treated by perturbation theory. Conclusions drawn from the results of our calculations are presented and discussed in Sec. VI. Appendixes in which certain results needed in the body of this paper are collected conclude this paper.

II. THE SCATTERING SYSTEM

Let us consider a free-standing metal film defined as follows (Fig. 2): vacuum in the regions $x_3 > \zeta(x_1)$ (region I) and $x_3 < -d$ (region III), and a metal characterized by an isotropic, frequency-dependent, complex, dielectric function $\epsilon(\omega)$ in the region $-d < x_3 < \zeta(x_1)$ (region II). The surface profile function $\zeta(x_1)$ is assumed to be a continuous, single-valued function of x_1, which is differentiable as many times as is necessary. In addition, we assume that $\zeta(x_1)$ is a stationary, Gaussian, stochastic process defined by the properties $\langle \zeta(x_1) \rangle = 0$, and

$$\langle \zeta(x_1)\zeta(x_1') \rangle = \delta^2 W(|x_1 - x_1'|) , \tag{2.1}$$

where the angular brackets denote an average over the ensemble of realizations of $\zeta(x_1)$, and $\delta = \langle \zeta^2(x_1) \rangle^{1/2}$ is the rms height of the surface. In numerical calculations, the Gaussian form

$$W(|x_1|) = \exp(-x_1^2/a^2) \tag{2.2}$$

will be used for the surface height correlation function, where a is called the transverse correlation length of the surface roughness.

We will use throughout this paper the Fourier integral representation of $\zeta(x_1)$,

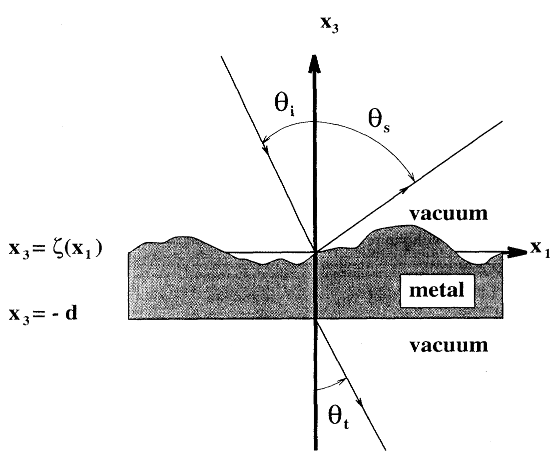

FIG. 2. The free-standing metal film studied in the present paper.

$$\zeta(x_1) = \int_{-\infty}^{\infty} \frac{dk}{2\pi} \hat{\zeta}(k) \exp(ikx_1) . \tag{2.3}$$

The Fourier coefficient $\hat{\zeta}(k)$ is also a Gaussian random process that possesses the following statistical properties:

$$\langle \hat{\zeta}(k) \rangle = 0 , \tag{2.4}$$

$$\langle \hat{\zeta}(k)\hat{\zeta}(k') \rangle = 2\pi\delta(k+k')\delta^2 g(|k|) , \tag{2.5}$$

where the form of the power spectrum of the surface roughness $g(|k|)$ corresponding to the choice of $W(|x_1|)$ in Eq. (2.2) is

$$g(|k|) = \pi^{1/2} a \exp(-k^2a^2/4) . \tag{2.6}$$

III. SURFACE PLASMON POLARITONS

Before going on to the case of a rough vacuum-metal interface, we shall briefly study the existence of eigenmodes in the case of a perfectly flat, free-standing metallic film for which $\zeta(x_1) \equiv 0$. These modes, called surface plasmon polaritons (SPP), play an important role in the scattering theory addressed in this paper.

A surface plasmon polariton is described by a p-polarized electromagnetic field whose magnetic vector has the form

$$\mathbf{H}(x;t) = (0, H_2(x_1,x_3|\omega), 0) \exp(-i\omega t) . \tag{3.1}$$

$H_2(x_1,x_3|\omega)$ is given by

$$H_2^{(\mathrm{I})}(x_1,x_3|\omega) = Ae^{iqx_1} \exp\left[-\beta_0(q,\omega)\left[x_3 + \frac{d}{2}\right]\right] \tag{3.2}$$

in region I, either

$$H_2^{(\mathrm{II})}(x_1,x_3|\omega) = Be^{iqx_1} \cosh\beta(q,\omega)\left[x_3 + \frac{d}{2}\right] \tag{3.3a}$$

or

$$H_2^{(\mathrm{II})}(x_1,x_3|\omega) = Be^{iqx_1} \sinh\beta(q,\omega)\left[x_3 + \frac{d}{2}\right] \tag{3.3b}$$

in region II, and

$$H_2^{(\mathrm{III})}(x_1,x_3|\omega) = Ae^{iqx_i} \exp\left[\beta_0(q,\omega)\left[x_3 + \frac{d}{2}\right]\right] \tag{3.4}$$

in region III, where $\beta_0(q,\omega) = [q^2 - (\omega^2/c^2)]^{1/2}$ and $\beta(q,\omega) = [q^2 - \epsilon(\omega)(\omega^2/c^2)]^{1/2}$. In writing Eqs. (3.2)–(3.4), we have explicitly exploited the symmetry of the system with respect to the plane $x_3 = -d/2$.

By imposing the boundary conditions at $x_3 = 0$

$$H_2^{(\mathrm{I})}(x_2,x_3|\omega)|_{x_3=0} = H_2^{(\mathrm{II})}(x_1,x_3|\omega)|_{x_3=0} , \tag{3.5a}$$

$$\frac{\partial}{\partial x_3} H_2^{(\mathrm{I})}(x_1,x_3|\omega)|_{x_3=0} = \frac{1}{\epsilon(\omega)} \frac{\partial}{\partial x_3} H_2^{(\mathrm{II})}(x_1,x_3|\omega)|_{x_3=0} \tag{3.5b}$$

to expressions (3.2) and (3.3a), and (3.2) and (3.3b), we are led to the following equations, respectively:

$$\epsilon(\omega)\beta_0(q,\omega)+\beta(q,\omega)\tanh\beta(q,\omega)\frac{d}{2}=0\ , \tag{3.6a}$$

$$\epsilon(\omega)\beta_0(q,\omega)+\beta(q,\omega)\coth\beta(q,\omega)\frac{d}{2}=0\ . \tag{3.6b}$$

Equations (3.6) are the dispersion relations for the p-polarized SPP supported by a free-standing metal film.

Let us assume that the dielectric function of the metal is given by Drude's expression $\epsilon(\omega)=1-\omega_p^2/\omega^2$, where ω_p is the plasma frequency of the electrons. Then for frequencies such that $\omega<\omega_p/\sqrt{2}$, Eqs. (3.6a) and (3.6b) each yield a single solution for the wave number q, hereafter called $q_1(\omega)$ and $q_2(\omega)$ (Fig. 3). On the other hand, for $\omega>\omega_p/\sqrt{2}$, Eq. (3.6a) has no solutions, whereas Eq. (3.6a) gives two different solutions, $q_1(\omega)$ and $q'_1(\omega)$, provided that the frequency does not exceed a certain maximum value.

Note that when the thickness of the film is sufficiently large, both Eqs. (3.6a) and (3.6b) tend to the same solvability condition, which in turn is the dispersion relation for SPP on a flat surface separating vacuum from a semi-infinite metal: $q=(\omega/c)\{\epsilon(\omega)/[\epsilon(\omega)+1]\}^{1/2}$. This physically means that, when the distance between the film surfaces is large compared to the spatial spread of the SPP inside the metal $[\beta(q,\omega)d\gg1]$, these SPP bound to each interface hardly interact with each other, and propagate similarly to the SPP at the interface between vacuum and a semi-infinite metal.

Nevertheless, we will focus in what follows on the case in which the metal film supports two distinct SPP excited through the roughness of the upper vacuum-film interface by a p-polarized incident beam of frequency $\omega<\omega_p/\sqrt{2}$. The mean thickness of the film d and the frequency ω will be chosen in such a way that the difference between the SPP wave numbers is significant.

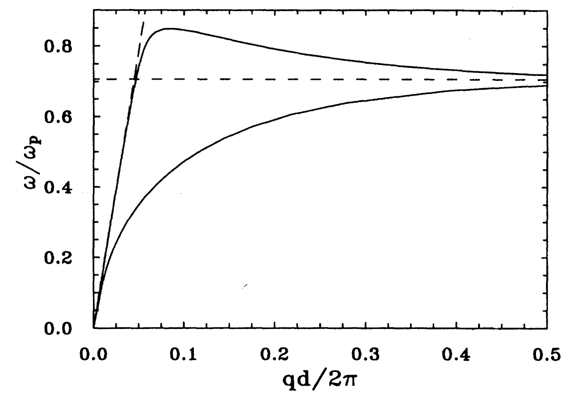

FIG. 3. The dispersion curves for the surface plasmon polaritons supported by the free-standing metal film depicted in Fig. 2, in the limit that the surface profile function $\zeta(x_1)$ vanishes identically, and the dielectric function of the metal has the Drude form $\epsilon(\omega)=1-(\omega_p^2/\omega^2)$.

IV. PERTURBATION THEORY

In this section, we develop a perturbation theory of the scattering and transmitted amplitudes up to third order in the surface profile function, which allows us to calculate the contributions to the mean differential reflection and transmission coefficients from the incoherent component of the scattered and transmitted wave that are valid through terms of fourth order in $\zeta(x_1)$. This perturbation theory gives physical insight into the effects we are interested in through the explicit analytic expressions it provides, and sheds light on the exact numerical simulation calculations addressed in Sec. IV. In addition, this approximation has proven successful in describing quantitatively the enhanced backscattering of electromagnetic waves from a one-dimensional, randomly rough, vacuum-metal interface on a semi-infinite metal.[6] Moreover, a similar approximation has been recently applied to the study of the scattering of electromagnetic (EM) waves from a dielectric film, with a random rough surface, on a perfectly conducting substrate.[7]

We consider a p-polarized electromagnetic wave of frequency ω that illuminates the surface $x_3=\zeta(x_1)$ from the vacuum region I $[x_3>\zeta(x_1)]$, and whose magnetic vector is written in the form of Eq. (3.1). The field amplitude $H_2(x_1,x_3|\omega)$ can be written in the form

$$H_2^{(\mathrm{I})}(x_1,x_3|\omega)=\exp[ikx_1-i\alpha_0(k,\omega)x_3]+\int_{-\infty}^{\infty}\frac{dq}{2\pi}R(q|k)\exp[iqx_1+i\alpha_0(q,\omega)x_3]\ , \tag{4.1}$$

$$H_2^{(\mathrm{II})}(x_1,x_3|\omega)=\int_{-\infty}^{\infty}\frac{dq}{2\pi}\exp(iqx_1)\{A(q|k)\exp[i\alpha(q,\omega)x_3]+B(q|k)\exp[-i\alpha(q,\omega)x_3]\}\ , \tag{4.2}$$

and

$$H_2^{(\mathrm{III})}(x_1,x_3|\omega)=\int_{-\infty}^{\infty}\frac{dq}{2\pi}T(q|k)\exp[iqx_1-i\alpha_0(q,\omega)(x_3+d)]\ , \tag{4.3}$$

in regions I, II, and III, respectively, where

$$\alpha_0(q,\omega)=\begin{cases}\left[\dfrac{\omega^2}{c^2}-q^2\right]^{1/2}, & q^2<\dfrac{\omega^2}{c^2} \quad (4.4a)\\[2ex] i\left[q^2-\dfrac{\omega^2}{c^2}\right]^{1/2}, & q^2>\dfrac{\omega^2}{c^2} \quad (4.4b)\end{cases}$$

and

$$\alpha(q,\omega)=\left[\epsilon(\omega)\frac{\omega^2}{c^2}-q^2\right]^{1/2},$$

$$\mathrm{Re}[\alpha(q,\omega)]>0\ ,\quad \mathrm{Im}[\alpha(q,\omega)]>0\ . \tag{4.5}$$

The contributions to the mean differential reflection and transmission coefficients from the incoherent components of the reflected and transmitted fields are given in terms of the reflection and transmission amplitudes $R(p|k)$ and $T(p|k)$ by

$$\left\langle\frac{\partial R_p}{\partial\theta_s}\right\rangle_{\mathrm{incoh}}=\frac{1}{L_1}\frac{\omega}{2\pi c}\frac{\cos^2\theta_s}{\cos\theta_0}\times[\langle|R(p|k)|^2\rangle-|\langle R(p|k)\rangle|^2]\ , \tag{4.6}$$

$$\left\langle\frac{\partial T_p}{\partial\theta_t}\right\rangle_{\mathrm{incoh}}=\frac{1}{L_1}\frac{\omega}{2\pi c}\frac{\cos^2\theta_t}{\cos\theta_0}\times[\langle|T(p|k)|^2\rangle-|\langle T(p|k)\rangle|^2]\ , \tag{4.7}$$

respectively, where L_1 is the length of the surface along the x_1 axis. The angles of incidence, scattering, and transmission are defined in the following manner:

$$k=\frac{\omega}{c}\sin\theta_0\ ,\quad p=\frac{\omega}{c}\sin\theta_s=\frac{\omega}{c}\sin\theta_t\ , \tag{4.8}$$

according to the conventions depicted in Fig. 2.

Our aim is to obtain the equations satisfied by $R(q|k)$ and $T(q|k)$ by introducing the magnetic field amplitudes Eqs. (4.1)–(4.3) into the corresponding boundary conditions at the film interfaces. First, we use the boundary conditions Eqs. (3.5) at $x_3=-d$ in order to express the coefficients $A(q|k)$ and $B(q|k)$, appearing in Eq. (4.2), in terms of the transmission amplitude $T(q|k)$, with the result that

$$A(q|k)=f_-(q,\omega)T(q|k)\ , \tag{4.9a}$$

$$B(q|k)=f_+(q,\omega)T(q|k)\ , \tag{4.9b}$$

where

$$f_\pm(q,\omega)=\frac{1}{2}\left[1\pm\epsilon(\omega)\frac{\alpha_0(q,\omega)}{\alpha(q,\omega)}\right]\exp[\mp i\alpha(q,\omega)d]\ . \tag{4.10}$$

We now introduce Eqs. (4.1) and (4.2), with the help of Eqs. (4.9), into the boundary conditions at $x_3=\zeta(x_1)$ (thus involving the Rayleigh hypothesis[8,9]),

$$H_2^{(\mathrm{I})}(x_1,x_3|\omega)|_{x_3=\zeta(x_1)}=H_2^{(\mathrm{II})}(x_1,x_3|\omega)|_{x_3=\zeta(x_1)}\ ,$$

$$\frac{\partial}{\partial n}H_2^{(\mathrm{I})}(x_1,x_3|\omega)|_{x_3=\zeta(x_1)}=\frac{1}{\epsilon(\omega)}\frac{\partial}{\partial n}H_2^{(\mathrm{II})}(x_1,x_3|\omega)|_{x_3=\zeta(x_1)}\ ,$$

where

$$\frac{\partial}{\partial n}\equiv\{1+[\zeta'(x_1)]^2\}^{-1/2}\left[-\zeta'(x_1)\frac{\partial}{\partial x_1}+\frac{\partial}{\partial x_3}\right]$$

is the normal derivative, and obtain

$$\exp[ikx_1-i\alpha_0(k,\omega)\zeta(x_1)]+\int_{-\infty}^{\infty}\frac{dq}{2\pi}R(q|k)\exp[iqx_1+i\alpha_0(q,\omega)\zeta(x_1)]$$
$$=\int_{-\infty}^{\infty}\frac{dq}{2\pi}T(q|k)\exp(iqx_1)\{f_-(q,\omega)\exp[i\alpha(q,\omega)\zeta(x_1)]+f_+(q,\omega)\exp[-i\alpha(q,\omega)\zeta(x_1)]\}\ , \tag{4.11}$$

and

$$[\zeta'(x_1)k+\alpha_0(k,\omega)]\exp[ikx_1-i\alpha_0(k,\omega)\zeta(x_1)]-\int_{-\infty}^{\infty}\frac{dq}{2\pi}R(q|k)[-\zeta'(x_1)q+\alpha_0(q,\omega)]\exp[iqx_1+i\alpha_0(q,\omega)\zeta(x_1)]$$
$$=-\frac{1}{\epsilon(\omega)}\int_{-\infty}^{\infty}\frac{dq}{2\pi}T(q|k)\exp(iqx_1)\{f_-(q,\omega)[-\zeta'(x_1)q+\alpha(q,\omega)]\exp[i\alpha(q,\omega)\zeta(x_1)]$$
$$+f_+(q,\omega)[-\zeta'(x_1)q-\alpha(q,\omega)]\exp[-i\alpha(q,\omega)\zeta(x_1)]\}\ . \tag{4.12}$$

These integral equations can be decoupled in such a way that a single integral equation for either $R(q|k)$ alone or $T(q|k)$ alone is obtained. In what follows, we use these decoupled integral equations to develop the perturbation calculations for reflection and transmission separately.

A. Reflection

If we multiply Eq. (4.11) by

$$e^{-ipx_1}\{f_-(p,\omega)[\zeta'(x_1)p+\alpha(p,\omega)]\exp[i\alpha(p,\omega)\zeta(x_1)]-f_+(p,\omega)[-\zeta'(x_1)p+\alpha(p,\omega)]\exp[-i\alpha(p,\omega)\zeta(x_1)]\}\ ,$$

and Eq. (4.12) by

$$\epsilon(\omega)e^{-ipx_1}\{f_-(p,\omega)\exp[i\alpha(p,\omega)\zeta(x_1)]+f_+(p,\omega)\exp[-i\alpha(p,\omega)\zeta(x_1)]\}\ ,$$

integrate both with respect to x_1, and add the resulting equations, we are led to

$$\int_{-\infty}^{\infty}\frac{dq}{2\pi}M_R(p|q)R(q|k)=N_R(p|k)\ , \tag{4.13}$$

where the functions $M_R(p|q)$ and $N_R(p|k)$ are defined by

$$\begin{aligned}M_R(p|q)={}&f_-(p,\omega)\left[\epsilon(\omega)\alpha_0(q,\omega)-\alpha(p,\omega)-[\epsilon(\omega)q+p]\frac{p-q}{\alpha_0(q,\omega)+\alpha(p,\omega)}\right]I[\alpha_0(q,\omega)+\alpha(p,\omega)|p-q]\\&+f_+(p,\omega)\left[\epsilon(\omega)\alpha_0(q,\omega)+\alpha(p,\omega)-[\epsilon(\omega)q+p]\frac{p-q}{\alpha_0(q,\omega)-\alpha(p,\omega)}\right]I[\alpha_0(q,\omega)-\alpha(p,\omega)|p-q]\ ,\end{aligned} \tag{4.14}$$

$$\begin{aligned}N_R(p|k)={}&f_-(p,\omega)\left[\alpha(p,\omega)+\epsilon(\omega)\alpha_0(k,\omega)+[p+\epsilon(\omega)k]\frac{p-k}{\alpha(p,\omega)-\alpha_0(k,\omega)}\right]I[\alpha(p,\omega)-\alpha_0(k,\omega)|p-k]\\&-f_+(p,\omega)\left[\alpha(p,\omega)-\epsilon(\omega)\alpha_0(k,\omega)+[p+\epsilon(\omega)k]\frac{p-k}{\alpha(p,\omega)+\alpha_0(k,\omega)}\right]I[-\alpha(p,\omega)-\alpha_0(k,\omega)|p-k]\ ,\end{aligned} \tag{4.15}$$

and $I(\gamma|Q)$ is

$$I(\gamma|Q)=\int_{-\infty}^{\infty}dx_1e^{-iQx_1}e^{i\gamma\zeta(x_1)}\ . \tag{4.16}$$

Equation (4.13) constitutes a single integral equation for the reflection amplitude that is the analog for the problem studied here of the reduced Rayleigh equation for the scattering amplitude obtained by Toigo *et al.* for the scattering of a *p*-polarized plane wave incident from the vacuum side on the one-dimensional, randomly rough surface of a semi-infinite metal.[10] We could base a small amplitude perturbation calculation of $R(q|k)$ on it, in a manner similar to what was done in Ref. 10. Instead, we modify Eq. (4.13) by employing the formalism of many-body perturbation theory calculations. First, we postulate that the reflection amplitude $R(q|k)$ obeys the following expression:[11]

$$\begin{aligned}R(p|k)={}&2\pi\delta(p-k)R_0(k,\omega)\\&-2iG_0(p,\omega)U_R(p/k)G_0(k,\omega)\alpha_0(k,\omega)\ .\end{aligned} \tag{4.17}$$

$R_0(k,\omega)$ is the Fresnel coefficient for the scattering of *p*-polarized electromagnetic waves from a free-standing metallic film with both metal-vacuum interfaces planar and parallel, namely,

$$R_0(k,\omega)=\frac{D_+(k,\omega)}{D_-(k,\omega)}\ , \tag{4.18}$$

where

$$D_\pm(k,\omega)=\Delta_+(k,\omega)\pm\frac{\alpha(k,\omega)}{\epsilon(\omega)\alpha_0(k,\omega)}\Delta_-(k,\omega)\ , \tag{4.19}$$

with

$$\Delta_\pm(k,\omega)=f_-(k,\omega)\pm f_+(k,\omega)\ . \tag{4.20}$$

The function $G_0(k,\omega)$ is the Green's function for the above-mentioned planar metal film, and can be shown to be given by

$$G_0(k,\omega)=\frac{i}{\alpha_0(k,\omega)D_-(k,\omega)}\ . \tag{4.21}$$

The reflection transition matrix $U_R(p|k)$ is postulated to satisfy the equations[11]

$$U_R(p|k)=V_R(p|k)+\int_{-\infty}^{\infty}\frac{dq}{2\pi}V_R(p|q)G_0(q,\omega)U_R(q|k) \tag{4.22a}$$

$$=V_R(p|k)+\int_{-\infty}^{\infty}\frac{dq}{2\pi}U_R(p|q)G_0(q,\omega)V_R(q|k)\ , \tag{4.22b}$$

where $V_R(p|k)$ is the reflection potential. By introducing Eq. (4.17) into Eq. (4.6), the contribution to the mean differential reflection coefficient from the incoherent component of the reflected field can be rewritten in terms of the reflection transition matrix as

$$\left\langle\frac{\partial R_p}{\partial\theta_s}\right\rangle_{\text{incoh}}=\frac{2}{\pi L_1}\left[\frac{\omega}{c}\right]^3\cos\theta_0\cos^2\theta_s|G_0(p,\omega)|^2[\langle|U_R(p|k)|^2\rangle-|\langle U_R(p|k)\rangle|^2]|G_0(k,\omega)|^2\ . \tag{4.23}$$

Therefore, we need to calculate $U_R(p|k)$ with the help of the preceding formulation and the integral equation containing the information provided by the boundary conditions.

By using Eq. (4.17) in Eq. (4.13), the equation satisfied by $U_R(q|k)$ is obtained:

$$\int_{-\infty}^{\infty}\frac{dq}{2\pi}M_R(p|q)G_0(q,\omega)U_R(q|k)=\frac{M_R(p|k)R_0(k,\omega)-N_R(p|k)}{2i\alpha_0(k,\omega)G_0(k,\omega)}\ . \tag{4.24}$$

It turns out to be more convenient to work with the reflection potential $V_R(q|k)$ as defined in Eqs. (4.22). If we replace $U_R(q|k)$ in Eq. (4.24) by the right-hand side of Eq. (4.22b), we obtain

$$\int_{-\infty}^{\infty}\frac{dq}{2\pi}M_R(p|q)G_0(q,\omega)V_R(q|k)+\int_{-\infty}^{\infty}\frac{dq}{2\pi}\int_{-\infty}^{\infty}\frac{dr}{2\pi}M_R(p|q)G_0(q,\omega)U_R(q|r)G_0(r,\omega)V_R(r|k)$$
$$=\frac{M_R(p|k)R_0(k,\omega)-N_R(p|k)}{2i\alpha_0(k,\omega)G_0(k,\omega)} . \tag{4.25}$$

On employing Eq. (4.24) in the second term on the left-hand side of Eq. (4.25), and Eqs. (4.18) and (4.21), the equation satisfied by the reflection potential $V_R(q|k)$ is finally obtained:

$$\int_{-\infty}^{\infty}\frac{dq}{2\pi}A(p|q)V_R(q|k)=B(p|k) , \tag{4.26}$$

where

$$A(p|q)=\frac{1}{2i\alpha_0(q,\omega)}\times\left[M_R(p|q)\frac{D_+(q,\omega)-2}{D_-(q,\omega)}-N_R(p|q)\right] , \tag{4.27}$$

$$B(p|k)=\tfrac{1}{2}[N_R(p|k)D_-(k,\omega)-M_R(p|k)D_+(k,\omega)] . \tag{4.28}$$

Equation (4.26) constitutes the basis of our perturbation theory calculation in reflection.

We seek $V_R(p|k)$ as an expansion in powers of the surface profile function $\zeta(x_1)$,

$$V_R(p|k)=\sum_{n=1}^{\infty}V_R^{(n)}(p|k) , \tag{4.29}$$

where the superscript denotes the order of the corresponding term in $\zeta(x_1)$. Similarly, we expand $A(p|q)$ and $B(p|q)$, Eqs. (4.27) and (4.28),

$$A(p|q)=\sum_{n=0}^{\infty}A^{(n)}(p|q) , \tag{4.30}$$

$$B(p|q)=\sum_{n=0}^{\infty}B^{(n)}(p|q) , \tag{4.31}$$

with the help of the expansion of $I(\gamma|Q)$, Eq. (4.16), in the form

$$I(\gamma|Q)=\sum_{n=0}^{\infty}\frac{(i\gamma)^n}{n!}\hat{\zeta}^n(Q) , \tag{4.32}$$

where

$$\hat{\zeta}^{(n)}(Q)=\int_{-\infty}^{\infty}dx_1e^{-iQx_1}\zeta^n(x_1) . \tag{4.33}$$

By introducing Eqs. (4.29)–(4.32) into Eq. (4.26), and then equating in the resulting equation terms of the same order in $\zeta(x_1)$, we obtain the following recurrence relation for the $\{V_R^{(n)}(p|k)\}$:

$$V_R^{(1)}(p|k)=-\frac{i}{\epsilon(\omega)}B^{(1)}(p|k) , \tag{4.34a}$$

$$V_R^{(n)}(p|k)-\frac{i}{\epsilon(\omega)}\sum_{r=1}^{n-1}\int_{-\infty}^{\infty}\frac{dq}{2\pi}A^{(n-r)}(p|q)V_R^{(r)}(q|k)=-\frac{i}{\epsilon(\omega)}B^{(n)}(p|k) , \quad n\geq 2 , \tag{4.34b}$$

where we have used the results that

$$A^{(0)}(p|q)=2\pi\delta(p-q)i\epsilon(\omega) , \tag{4.35}$$

$$B^{(0)}(p|k)=0 . \tag{4.36}$$

Since, for our purpose, it suffices to consider terms of $V_R(p|k)$ through third order in $\zeta(x_1)$, it is evident from Eqs. (4.34) that we only need the terms up to second order in the expansion of $A(p|q)$ [Eq. (4.30)], and up to third order in the expansion of $B(p|k)$ [Eq. (4.31)]. These terms can be easily calculated from Eqs. (4.14), (4.15), (4.27), (4.28), and (4.32). By making use of these results in the recurrence relation, Eqs. (4.34), the three leading terms in the expansion of $V_R(p|k)$ are obtained:

$$V_R^{(1)}(p|k)=v_R^{(1)}(p|k)\hat{\zeta}^{(1)}(p-k) , \tag{4.37a}$$

$$V_R^{(2)}(p|k)=\int_{-\infty}^{\infty}\frac{dq}{2\pi}v_R^{(2)}(p|q|k)\times\hat{\zeta}^{(1)}(p-q)\hat{\zeta}^{(1)}(q-k) , \tag{4.37b}$$

$$V_R^{(3)}(p|k)=\int_{-\infty}^{\infty}\frac{dq}{2\pi}\int_{-\infty}^{\infty}\frac{dr}{2\pi}v_R^{(3)}(p|q|r|k)\hat{\zeta}^{(1)}(p-q)\times\hat{\zeta}^{(2}(q-r)\hat{\zeta}^{(1)}(r-k) , \tag{4.37c}$$

where we have introduced the functions $v_R^{(1)}(p|k)$, $v_R^{(2)}(p|q|k)$, and $v_R^{(3)}(p|q|r|k)$. These functions are displayed in Appendix A, and their properties that ensure the reciprocity of the reflection potential in each order in $\zeta(x_1)$ are discussed: $V^{(n)}(p|k)=V^{(n)}(-k|-p)$.

Our aim is to calculate the mean differential reflection coefficient as given by Eq. (4.23), which depends in turn on the transition matrix $U_R(p|k)$. Therefore, we expand $U_R(p|k)$ in powers of $\zeta(x_1)$,

$$U_R(p|k)=\sum_{n=1}^{\infty}U_R^{(n)}(p|k) , \tag{4.38}$$

and use Eqs. (4.22a) and (4.29) to express the $\{U_R^{(n)}(p|k)\}$ in terms of the $\{V_R^{(n)}(p|k)\}$. It is found that the three leading terms are given by

$$U_R^{(1)}=V_R^{(1)} , \tag{4.39a}$$

$$U_R^{(2)}=V_R^{(2)}+V_R^{(1)}G_0V_R^{(1)} , \tag{4.39b}$$

$$U_R^{(3)}=V_R^{(3)}+V_R^{(2)}G_0V_R^{(1)}+V_R^{(1)}G_0V_R^{(2)} + V_R^{(1)}G_0V_R^{(1)}G_0V_R^{(1)} , \tag{4.39c}$$

where the notation is such that a product of $V_R^{(n)}$ terms means integration with respect to the inner argument. Finally, the incoherent contribution to the mean differential reflection coefficient is obtained by using Eqs. (4.37)–(4.39) in Eq. (4.23). Upon considering the statistical properties of the Gaussian random process $\zeta(x_1)$, Eqs. (2.4)–(2.6), and keeping terms up to fourth order in $\zeta(x_1)$ in the resulting expression, we are led to

$$\left\langle\frac{\partial R_p}{\partial\theta_s}\right\rangle_{\text{incoh}}=\frac{2}{\pi}\left[\frac{\omega}{c}\right]^3\cos^2\theta_s\cos\theta_0|G_0(p,\omega)|^2 \times\{I_R^{(1-1)}(p|k)+I_R^{(2-2)L}(p|k) +I_R^{(2-2)C}(p|k)+I_R^{(1-3)}(p|k)\} \times|G_0(k,\omega)|^2 . \tag{4.40}$$

In Eq. (4.40), $I_R^{(1-1)}(p|k)$ yields the second-order contribution, and $I_R^{(2-2)L}$, $I_R^{(2-2)C}$, and $I_R^{(1-3)}$ give the contributions of fourth order in $\zeta(x_1)$ from, respectively, the ladder term, the maximally crossed term, and the contribution arising from the products of the terms containing $U_R^{(1)}$ and $U_R^{(3)}$. These contributions are given as functions of $v_R^{(1)}$, $v_R^{(2)}$, and $v_R^{(3)}$, Eqs. (A1)–(A5), in Appendix B.

B. Transmission

By multiplying Eq. (4.11) by

$$[\alpha_0(p,\omega)+p\zeta'(x_1)]\exp[-ipx_1+i\alpha_0(p,\omega)\zeta(x_1)]$$

and Eq. (4.12) by

$$\exp[-ipx_1+i\alpha_0(p,\omega)\zeta(x_1)] ,$$

integrating both with respect to x_1, and adding the resulting equations, we obtain the following single integral equation for the transmission amplitude $T(p|k)$ alone:

$$\int_{-\infty}^{\infty}\frac{dq}{2\pi}M_T(p|q)T(q|k)=N_T(p|k) . \tag{4.41}$$

The functions $M_T(p|q)$ and $N_T(p|k)$ are given by

$$M_T(p|q)=\frac{f_-(p,\omega)}{\epsilon(\omega)}\left[\epsilon(\omega)\alpha_0(p,\omega)-\alpha(q,\omega)+[\epsilon(\omega)p+q]\frac{p-q}{\alpha_0(p,\omega)+\alpha(q,\omega)}\right]I[\alpha_0(p,\omega)+\alpha(q,\omega)|p-q] + \frac{f_+(p,\omega)}{\epsilon(\omega)}\left[\epsilon(\omega)\alpha_0(p,\omega)+\alpha(q,\omega)+[\epsilon(\omega)p+q]\frac{p-q}{\alpha_0(p,\omega)-\alpha(q,\omega)}\right]I[\alpha_0(p,\omega)-\alpha(q,\omega)|p-q] , \tag{4.42}$$

$$N_T(p|k)=\left[\alpha_0(p,\omega)+\alpha_0(k,\omega)+\frac{p^2-k^2}{\alpha_0(p,\omega)-\alpha_0(k,\omega)}\right]I[\alpha_0(p,\omega)-\alpha_0(k,\omega)|p-k] , \tag{4.43}$$

where $I(\gamma|Q)$ has been defined in Eq. (4.16). Equation (4.41) is the analog for the problem being studied here of the reduced Rayleigh equation for the amplitude of the transmitted field when a p-polarized plane wave is incident from the vacuum side on a one-dimensional, randomly rough surface of a semi-infinite metal.[10]

Let us rewrite Eqs. (4.42) and (4.43) by making use of the equations

$$I(\gamma|Q)=2\pi\delta(Q)+i\gamma J(\gamma|Q) , \tag{4.44}$$

$$J(\gamma|Q)=\int_{-\infty}^{\infty}dx_1e^{-iQx_1}\frac{e^{i\gamma\zeta(x_1)}-1}{i\gamma} , \tag{4.45}$$

with the result that

$$M_T(p|q)=2\pi\delta(p-q)\alpha_0(p,\omega)D_-(p,\omega) +i\frac{\epsilon(\omega)-1}{\epsilon(\omega)}\{f_-(q,\omega)[\alpha_0(p,\omega)\alpha(q,\omega)-pq]J[\alpha_0(p,\omega)+\alpha(q,\omega)|p-q] -f_+(q,\omega)[\alpha_0(p,\omega)\alpha(q,\omega)+pq]J[\alpha_0(p,\omega)-\alpha(q,\omega)|p-q]\} \tag{4.46a}$$

$$=2\pi\delta(p-q)\alpha_0(p,\omega)D_-(p,\omega)-iM_T'(p|q) , \tag{4.46b}$$

$$N_T(p|k)=2\pi\delta(p-k)2\alpha_0(k,\omega) . \tag{4.47}$$

Proceeding in the same way as in Sec. IV A, we introduce the formalism of many-body scattering theory by postulating that the transmission amplitude $T(p|k)$ is of the form

$$T(p|k)=2\pi\delta(p-k)T_0(k,\omega) -2iG_0(p,\omega)U_T(p|k)G_0(k,\omega)\alpha_0(k,\omega) . \tag{4.48}$$

$T_0(k,\omega)$ is the Fresnel coefficient for the transmission of

p-polarized EM waves through a free-standing metal film with planar, parallel interfaces,

$$T_0(k,\omega)=\frac{2}{D_-(k,\omega)} ; \tag{4.49}$$

$G_0(k,\omega)$ is the Green's function defined in Eq. (4.21), and $U_T(p|k)$ corresponds to the transmission transition matrix, which is in turn postulated to satisfy

$$U_T(p|k)=V_T(p|k)+\int_{-\infty}^{\infty}\frac{dq}{2\pi}V_T(p|q)G_0(q,\omega)U_T(q|k) \tag{4.50a}$$

$$=V_T(p|k)+\int_{-\infty}^{\infty}\frac{dq}{2\pi}U_T(p|q)G_0(q,\omega)V_T(q|k) , \tag{4.50b}$$

where $V_T(p|k)$ is the transmission potential. Then the contribution to the mean differential transmission coefficient from the incoherent component of the transmitted field, Eq. (4.7), depends on $U_T(p|k)$ through the equation

$$\left\langle\frac{\partial T_p}{\partial\theta_t}\right\rangle_{\text{incoh}}=\frac{2}{\pi L_1}\left[\frac{\omega}{c}\right]^3\cos^2\theta_t\,\cos\theta_0|G_0(p,\omega)|^2 \times[\langle|U_T(p|k)|^2\rangle-|\langle U_T(p|k)\rangle|^2] \times|G_0(k,\omega)|^2 . \tag{4.51}$$

In order to obtain the integral equation satisfied by $U_T(p|k)$, we substitute Eq. (4.48) in Eq. (4.41) with the result

$$\int_{-\infty}^{\infty}\frac{dq}{2\pi}M_T(p|q)G_0(q,\omega)U_T(q|k) =\frac{M_T(p|k)T_0(k,\omega)-N_T(p|k)}{2i\alpha_0(k,\omega)G_0(k,\omega)} . \tag{4.52}$$

It what follows, instead of following the procedure used in Sec. IV A, we rewrite Eq. (4.52) with the help of Eqs. (4.21), (4.46b), (4.47), and (4.49), thus arriving at

$$U_T(p|k)=M_T'(p|k)+\int_{-\infty}^{\infty}\frac{dq}{2\pi}M_T'(p|q)G_0(q,\omega)U_T(q|k) . \tag{4.53}$$

Consequently, on comparing this equation with Eq. (4.50a) it follows that the transmission potential is given in the closed form

$$V_T(p|k)=M_T'(p|k) =\frac{\epsilon(\omega)-1}{\epsilon(\omega)}\{f_-(k,\omega)[pk-\alpha_0(p,\omega)\alpha(k,\omega)]J[\alpha_0(p,\omega)+\alpha(k,\omega)|p-k] +f_+(k,\omega)[pk+\alpha_0(p,\omega)\alpha(k,\omega)]J[\alpha_0(p,\omega)-\alpha(k,\omega)|p-k]\} . \tag{4.54}$$

This simplifies notably our perturbation theory calculations, for it is straightforward to show that the expansion

$$V_T(p|k)=\sum_{n=1}^{\infty}V_T^{(n)}(p|k) \tag{4.55}$$

leads, with the help of Eqs. (4.32) and (4.44) to

$$V_T^{(n)}(p|k)=i^{n-1}\frac{\epsilon(\omega)-1}{\epsilon(\omega)}\hat{\zeta}^{(n)}(p-k)\{f_-(k,\omega)[pk-\alpha_0(p,\omega)\alpha(k,\omega)][\alpha_0(p,\omega)+\alpha(k,\omega)]^{n-1} +f_+(k,\omega)[pk+\alpha_0(p,\omega)\alpha(k,\omega)][\alpha_0(p,\omega)-\alpha(k,\omega)]^{n-1}\} \tag{4.56a}$$

$$\equiv v_T^{(n)}(p|k)\hat{\zeta}^{(n)}(p-k) . \tag{4.56b}$$

Therefore, keeping in mind that the three leading terms in the expansion of the transition matrix

$$U_T(p|k)=\sum_{n=1}^{\infty}U_T^{(n)}(p|k) \tag{4.57}$$

are related to the corresponding terms in the expansion of $V_T(p|k)$ [Eq. (4.56)] through expressions formally equal to Eqs. (4.39), we can write $\langle\partial T_p/\partial\theta_t\rangle_{\text{incoh}}$ through terms of fourth order in $\zeta(x_1)$ in the form

$$\left\langle\frac{\partial T_p}{\partial\theta_t}\right\rangle_{\text{incoh}}=\frac{2}{\pi}\left[\frac{\omega}{c}\right]^3\cos^2\theta_t\,\cos\theta_0|G_0(p,\omega)|^2 \times\{I_T^{(1-1)}(p|k)+I_T^{(2-2)L}(p|k)+I_T^{(2-2)C}(p|k)+I_T^{(1-3)}(p|k)\}|G_0(k,\omega)|^2 . \tag{4.58}$$

The superscripts of the functions $I_T^{(1-1)}$, $I_T^{(2-2)L}$, $I_T^{(2-2)C}$, and $I_T^{(1-3)}$ have the same meanings as those for the functions $I_R^{(1-1)}$, $I_R^{(2-2)L}$, $I_R^{(2-2)C}$, and $I_R^{(1-3)}$. In fact, the functions $I_T^{(1-1)}$, $I_T^{(2-2)L}$, $I_T^{(2-2)C}$, and $I_R^{(1-3)}$ are given by expressions formally identical to those defining the functions $I_R^{(1-1)}$, $I_R^{(2-2)L}$, $I_R^{(2-2)C}$, and $I_R^{(1-3)}$, obtained by replacing $v_R^{(1)}$, $v_R^{(2)}$, and $v_R^{(3)}$ in Eqs. (B1)–(B4) by $v_T^{(1)}$, $v_T^{(2)}$, and $v_T^{(3)}$, respectively, defined in Eqs. (4.56).

C. Results

We now present results of numerical calculations of $\langle \partial R_p/\partial\theta_s \rangle_{\rm incoh}$ and $\langle \partial T_p/\partial\theta_t \rangle_{\rm incoh}$ on the basis of the perturbation-theoretic analysis described above which has led to Eqs. (4.40) and (4.58). In particular, we choose a silver film whose upper vacuum-metal interface is a one-dimensional random surface (cf. Sec. II) with roughness parameters $\delta=5$ nm and $a=125$ nm. The wavelength of the p-polarized incident plane wave is $\lambda=457.9$ nm. For these choices for the values of δ, a, and λ, the conditions $\delta/\lambda \ll 1$ and $\delta/a \ll 1$ are well satisfied. The condition of small rms height stems from the fact that δ/λ is the small parameter in the perturbative expansion of the scattering coefficients, whereas $\delta/a \ll 1$ (condition of small rms slope) ensures the validity of the Rayleigh hypothesis.[12,13] Since the wavelength corresponds to a frequency below the value of $\omega_p/\sqrt{2}$ for silver, according to the discussion in Sec. III the metallic film supports two SPP whose wave numbers q_1 and q_2 are obtained from the dispersion relations (3.6a) and (3.6b), respectively; assuming that the mean thickness of the film is $d=35$ nm, the wave numbers thus obtained are $q_1=(\omega/c)1.028$ and $q_2=(\omega/c)1.194$.

In Fig. 4, the results for the angular dependence of the contributions to the mean differential reflection and transmission coefficients from the incoherent components of the reflected and transmitted field, respectively, are shown for normal incidence. In addition, the contributions coming from second-order terms alone and from the fourth-order terms alone are included. In reflection, Fig. 4(a), a well-defined backscattering peak is observed at $\theta_s=0°$; in addition, two sharp satellite peaks symmetrically placed at $\theta_s=\pm 9.6°$ are present. Likewise, in transmission, two similar satellite peaks are seen in Fig. 4(b) at angles $\theta_t=\pm 9.6°$ on each side of the antispecular transmission peak at $\theta_t=0°$. All these peaks stem from the fourth-order contribution, whereas the second-order contribution is structureless. It has been shown in the Introduction that the existence of degenerate eigenmodes in a random bounded medium may lead to the appearance of satellite peaks in the angular distribution of the intensity of the scattered field; the condition for the phase coherence of the multiply scattered trajectories mediated by eigenmodes with different wave vectors in the case that the bounded medium supports two guided waves with wave numbers $q_1(\omega)$ and $q_2(\omega)$ at the frequency ω of the incident plane wave predicts that these peaks should occur at scattering angles θ_s given by Eq. (1.8). Our system supports two degenerate SPP whose wave numbers, shown above, determine very accurately the positions of the satellite peaks in Fig. 4(a) through condition (1.8), thus confirming the explanation given for the occurrence of such peaks. A similar argument has been applied in the Introduction to predict the existence of satellite peaks in the angular distribution of the intensity of the incoherent component of the transmitted field, at transmission angles given by Eq. (1.7), in agreement with the results presented in Fig. 4(b). It should be noted that, when $q_1(\omega)=q_2(\omega)$, Eqs. (1.8) and (1.7) lead to enhanced backscattering and enhanced antispecular transmission, respectively.

Furthermore, we can split the fourth-order term in Fig. 4 into three components: ladder, maximally crossed, and (1-3). This is done in Fig. 5. As expected, the peaks appear only in the maximally crossed contribution, both in

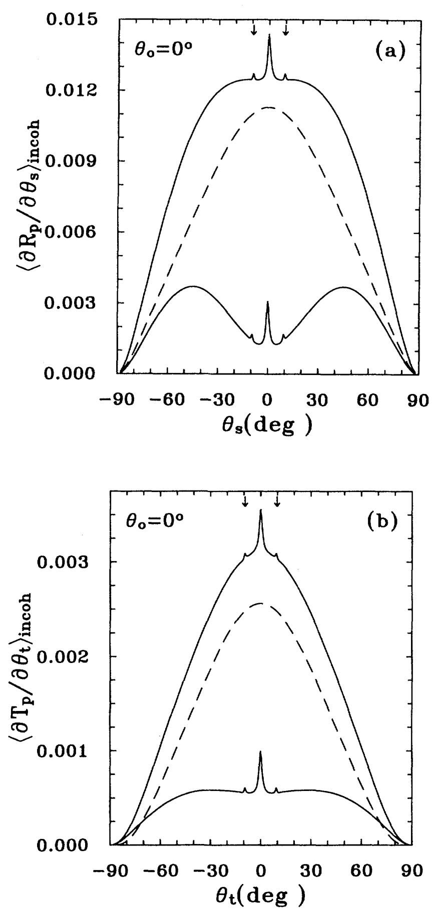

FIG. 4. Contribution through fourth order (upper solid curve) in the surface profile function to the mean differential scattering coefficient from the incoherent component of the scattered field for p-polarized electromagnetic waves of wavelength $\lambda=457.9$ nm incident at $\theta_0=0°$ on a free-standing silver film of mean thickness $d=35$ nm. The dielectric constant of silver at that wavelength is $\epsilon=-7.5+i0.24$. The one-dimensional, randomly rough, upper vacuum-metal interface is characterized by the parameters $\delta=5$ nm and $a=125$ nm. The second-order (dashed curve) and fourth-order (lower solid curve) contributions are also included. (a) Reflection; (b) transmission.

reflection and transmission, for this contribution accounts, indeed, for the interference effects between every doubly scattered trajectory and its time-reversed partner.

In order to observe the angular shift of those satellite peaks predicted by the conditions (1.8) and (1.7), we plot in Fig. 6 $\langle \partial R_p/\partial\theta_s \rangle_{\text{incoh}}$ and $\langle \partial T_p/\partial\theta_s \rangle_{\text{incoh}}$ as in Fig. 4, but for $\theta_0=5°$. Equations (1.8) and (1.7) give the following values for the positions of the peaks: $\theta_{s,t}=4.5°$ and $-14.7°$, which coincide with the angles obtained from the results shown in Figs. 4–6.

We should also mention the fact that, as Figs. 4 and 6 reveal, the total integrated contribution of second order in $\zeta(x_1)$ is substantially larger than the total fourth-order contribution, thus supporting the applicability of our perturbation theory for the roughness parameters considered here. Also, note that the total incoherent scattered energy is about 10 times larger than the total incoherent transmitted energy, both calculated up to fourth order in $\zeta(x_1)$.

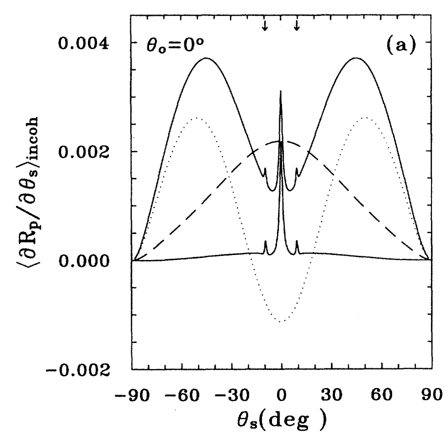

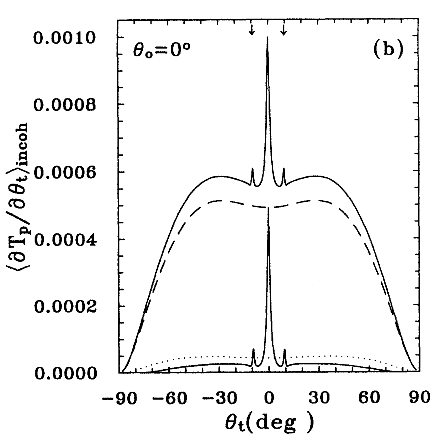

FIG. 5. Same as Fig. 4 but only for the fourth-order contribution (upper solid curve), including separately the ladder (dashed curve), crossed (lower solid curve), and (1-3) (dotted curve) terms.

V. NUMERICAL SIMULATION RESULTS

In this section we present Monte Carlo simulation results for the reflection and transmission of p-polarized EM waves from the same scattering system studied in Sec. IV C (see Fig. 2). The numerical procedure employed here corresponds to that applied in Ref. 2 to studies of the transmission of electromagnetic waves through thin metal films. Basically, the method consists of converting the scattering integral equations into matrix equations by means of a quadrature scheme that truncates the surface at a length L that is then divided into N equally spaced points. This is done for each realization of the random surface profile numerically generated by the method described in Appendix A of Ref. 14 in accordance with the assumed statistical properties (cf. Sec. II). Finally, $\langle \partial R_p/\partial\theta_s \rangle_{\text{incoh}}$ and $\langle \partial T_p/\partial\theta_t \rangle_{\text{incoh}}$ are obtained as averages of the results obtained from N_p realizations of the random surface. The p-polarized incident wave is assumed to be a Gaussian beam the half-width of whose intercept with the plane $x_3=0$ is g.

We would like to point out that, due to computational difficulties, no numerical simulation calculations have been carried out for the set of parameters used in obtaining the perturbation-theoretic results shown in Figs. 4–6.

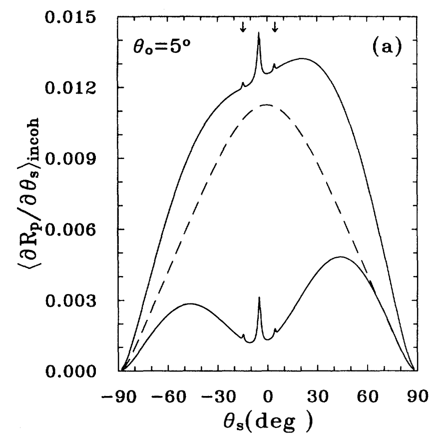

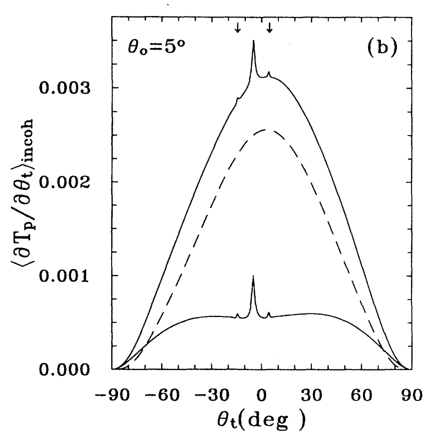

FIG. 6. Same as Fig. 4 but for $\theta_0=5°$.

There are two sources originating such difficulties. First, despite the large number of realizations over which the averages are made, the statistical noise can be of the order of or larger than the contribution from the incoherent scattered field to the mean differential reflection coefficient when the total incoherent scattered energy is considerably smaller than the total coherent scattered energy, as is the case for $\delta/\lambda \ll 1$. (The same applies in transmission.) Second, the diffraction of SPP at the surface edges may lead to unwanted effects because the SPP can propagate large distances on weakly rough surfaces.[15] Nevertheless, the numerical simulations provide rigorous results for rough surfaces for which the perturbation theory is inapplicable.

In what follows, we focus on a silver film with a random surface whose roughness parameters are $\delta=15$ nm and $a=100$ nm. The wavelength of the incident beam is $\lambda=394.7$ nm. The values of the numerical parameters are $L=12.6$ μm, $g=L/4$, $N=400$, and $N_p=1500$. The contributions to the mean differential reflection and transmission coefficients from the incoherent components of the scattered and transmitted field, respectively, are shown in Fig. 7 for an angle of incidence $\theta_0=0°$ and the mean film thickness $d=48$ nm. The vertical lines mark the positions of the satellite peaks as predicted by the conditions (1.8) and (1.7), with the use of the values of $q_1(\omega)$ and $q_2(\omega)$ obtained from Eqs. (3.6): $q_1(\omega)=(\omega/c)1.073$ and $q_2(\omega)=(\omega/c)1.267$. In addition to the enhanced backscattering and antispecular transmission peaks at $\theta_s=\theta_t=0°$, we observe two satellite peaks at $\theta_{s,t}=\pm 11.2°$, which coincide very accurately with the expected positions. In order to make sure that those peaks do not appear due to either the statistical noise or the subsidiary maxima associated with enhanced backscattering and antispecular transmission phenomena at normal incidence, we could vary either the angle of incidence or the mean thickness of the film, keeping the roughness parameters fixed. The first solution has been demonstrated to be unfeasible, at least in reflection, as regards a scattering system consisting of a dielectric film on a perfectly conducting substrate;[7] the reason is the rapid disappearance of the peak at $\theta_s=\theta_-$ on moving θ_0 away from normal incidence. On the other hand, varying d produces a change in the wave vectors $q_1(\omega)$ and $q_2(\omega)$ of the SPP which should in turn modify the positions of the satellite peaks following Eqs. (1.7) and (1.8). This is shown in Figs. 8 and 9 for a mean thickness $d=59$ and 68 nm, respectively: In the former case $q_1(\omega)=(\omega/c)1.092$ and $q_2(\omega)=(\omega/c)1.217$, whereas in the latter case $q_1(\omega)=(\omega/c)1.104$ and $q_1(\omega)=(\omega/c)1.193$, so that the peaks now appear at $\theta_{s,t}=\pm 7.2°$ in Fig. 8 and at $\theta_{s,t}=\pm 5.1°$ in Fig. 9, both in reflection and transmission, confirming our former reasoning. In this respect, note that the widths of the enhanced backscattering and antispecular transmission peaks are not altered by the change of d (see Figs. 7–9), since we have not changed the correlation length a (which determines their widths through the ratio λ/a).[16]

Finally, it should be pointed out that the numerical simulations, unlike the perturbation theory calculations of Sec. IV, take into account all orders of scattering. Therefore, this affects the values of the wave vectors of the SPP, which were worked out on the assumption of a metal film with planar parallel interfaces (cf. Sec. III). Nevertheless, since the values for $q_1(\omega)$ and $q_2(\omega)$ thus obtained permit accurately predicting the positions of the satellite peaks encountered in the numerical calculations through Eqs. (1.7) and (1.8), it is evident that the difference $q_2(\omega)-q_1(\omega)$ is not substantially modified by the presence of roughness for our choices of δ and a.

VI. CONCLUSIONS

In this paper, we have found features in the angular dependence of the intensity of incoherently scattered and transmitted electromagnetic waves in a system consisting of a free-standing silver film with a randomly rough illuminated surface. The mean thickness of the film must be such that, in the absence of roughness, it supports two

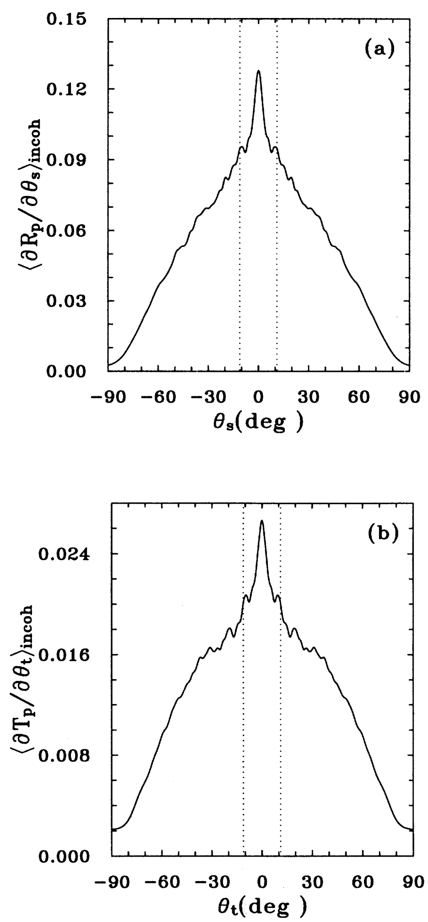

FIG. 7. Computer simulation results for the differential scattering coefficient for the scattering of a p-polarized beam from a one-dimensional random surface on a free-standing silver film of thickness $d=48$ nm. $\theta_0=0°$, $\delta=15$ nm, $a=100$ nm, $\lambda=394.7$ nm, $\epsilon=-4.28+i0.21$, $L=12.6$ μm, $g=L/4$, $N=400$, and $N_p=1500$. The vertical dashed lines indicate the scattering angles at which the satellite peaks occur according to Eq. (1.7) and (1.8). (a) Reflection; (b) transmission.

degenerate SPP which have, at a given frequency of the incoming beam, sufficiently different values of their wave numbers. Under these conditions, we observe two satellite peaks about the enhanced backscattering peak in reflection, and two satellite peaks about the enhanced transmission peak in transmission; the positions of these peaks are predicted by Eqs. (1.8) and (1.7), respectively, which result from a simple argument based on the phase coherence condition for multiply scattered trajectories mediated by degenerate SPP. Two approaches have been used to calculate the contributions to the mean differential reflection and transmission coefficients from the incoherent components of the reflected and transmitted field, respectively. On the one hand, a perturbation theory up to fourth order in the surface profile function $\zeta(x_1)$ has been developed which corroborates the occurrence of such peaks in the maximally crossed, double scattering contribution. On the other hand, numerical simulations have been carried out showing the existence of the satellite peaks without the constraints of small rms height δ/λ and small rms slope $\sqrt{2}\delta/a$, required for the validity of the perturbation-theoretic calculations.[12,13]

From a methodological standpoint the single integral equations (4.13) and (4.41) for the scattering and transmission amplitude derived in this paper should simplify future perturbative studies of the reflection and transmission of electromagnetic waves through free-standing films whose illuminated surface is rough, which could be dielectric films capable of supporting more than two guided waves, as well as metal films. These equations, and the many-body perturbation-theoretic formulation of the scattering and transmission problems based on them presented here, could also serve as the starting point for an infinite-order perturbation theory calculation of the intensities of the scattered and transmitted fields, as was done in Ref. 7. Finally, we note that although Eqs. (4.13) and (4.41) were obtained on the assumption that it is the illuminated surface of the film that is the randomly rough surface, while the back surface is planar, the same approach can be used to obtain analogous equations in the case that the illuminated surface is planar, while it is the back surface that is randomly rough.

ACKNOWLEDGMENTS

This work was supported in part by Army Research Office Grant No. DAAL03-92-G-0239. It was also sup-

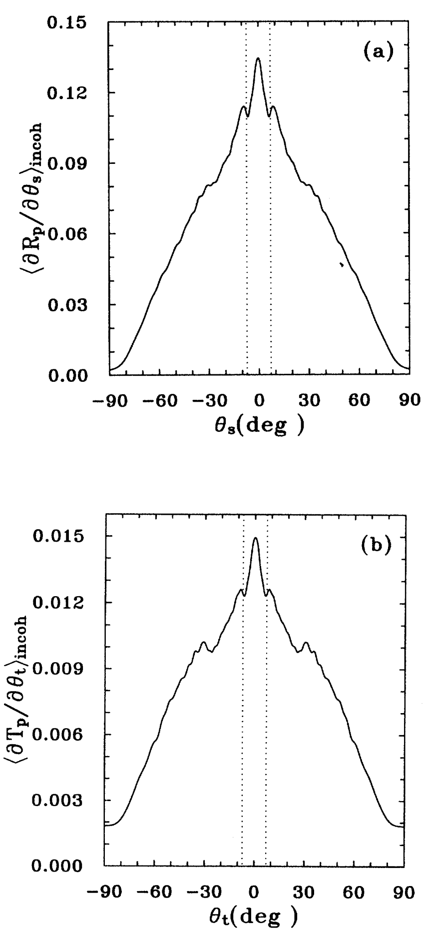

FIG. 8. Same as Fig. 7 but for $d = 59$ nm.

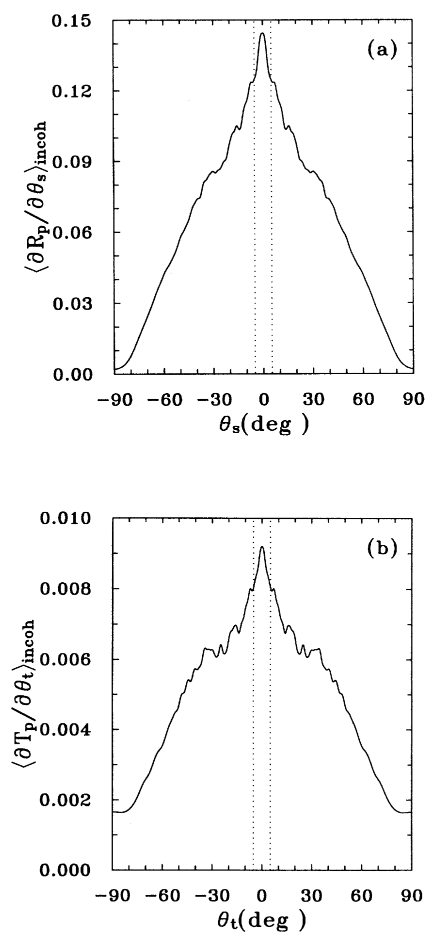

FIG. 9. Same as Fig. 7 but for $d = 68$ nm.

ported by the University of California, Irvine, through an allocation of computer time. J.A.S.G. acnowledges a grant from the Consejo Superior de Investigaciones Científicas.

APPENDIX A

The functions $v_R^{(1)}(p|k)$, $v_R^{(2)}(p|q|k)$, and $v_R^{(3)}(p|q|r|k)$ appearing in Eqs. (4.37) are given by

$$v_R^{(1)}(p|k)=\left[\frac{\epsilon(\omega)-1}{\epsilon(\omega)}\right]\left[pk\Delta_+(p,\omega)\Delta_+(k,\omega)-\frac{\alpha(p,\omega)\alpha(k,\omega)}{\epsilon(\omega)}\Delta_-(p,\omega)\Delta_-(k,\omega)\right], \tag{A1}$$

$$\begin{aligned} v_R^{(2)}(p|q|k)=&\frac{i}{2}\left[\frac{\epsilon(\omega)-1}{\epsilon(\omega)}\right]\{\alpha(p,\omega)[pk-\alpha_0^2(k,\omega)]\Delta_-(p,\omega)\Delta_+(k,\omega)\\ &\qquad+\alpha(k,\omega)[pk-\alpha_0^2(p,\omega)]\Delta_+(p,\omega)\Delta_-(k,\omega)\}\\ &+\left[\frac{\epsilon(\omega)-1}{\epsilon(\omega)}\right]^2 G_0(q,\omega)\left\{pq^2k[1-\Delta_+(q,\omega)]\Delta_+(p,\omega)\Delta_+(q,\omega)\Delta_+(k,\omega)\right.\\ &\qquad+\frac{\alpha(p,\omega)\alpha(q,\omega)\alpha(k,\omega)}{\epsilon(\omega)}\left[\alpha_0(q,\omega)-\frac{\alpha(q,\omega)}{\epsilon(\omega)}\Delta_-(q,\omega)\right]\\ &\qquad\times\Delta_-(p,\omega)\Delta_-(q,\omega)\Delta_-(k,\omega)+q\Delta_+(q,\omega)\left[\frac{\alpha(q,\omega)}{\epsilon(\omega)}\Delta_-(q,\omega)-\alpha_0(q,\omega)\right]\\ &\qquad\left.\times[p\alpha(k,\omega)\Delta_+(p,\omega)\Delta_-(k,\omega)+k\alpha(p,\omega)\Delta_-(p,\omega)\Delta_+(k,\omega)]\right\}, \end{aligned} \tag{A2}$$

$$\begin{aligned} v_R^{(3)}(p|q|r|k)=&-\frac{1}{6}\left[\frac{\epsilon(\omega)-1}{\epsilon(\omega)}\right]\left\{\Delta_+(p,\omega)\Delta_+(k,\omega)\left\{\left[2\epsilon(\omega)\frac{\omega^2}{c^2}-\frac{pk}{2}\left[3-\frac{1}{\epsilon(\omega)}\right]\right](p^2+k^2)\right.\right.\\ &\qquad\left.-\left[2-\frac{1}{\epsilon(\omega)}\right]p^2k^2+2\epsilon(\omega)\frac{\omega^2}{c^2}pk-2\epsilon(\omega)\frac{\omega^4}{c^4}\right\}\\ &\qquad\left.+\Delta_-(p,\omega)\Delta_-(k,\omega)\alpha(p,\omega)\alpha(k,\omega)\left[\frac{1}{2}\left[1+\frac{1}{\epsilon(\omega)}\right](p^2+k^2)+2pk-2\frac{\omega^2}{c^2}\right]\right\}\\ &-\frac{i}{2}\left[\frac{\epsilon(\omega)-1}{\epsilon(\omega)}\right]^2[G_0(q,\omega)u_{12}(p|q|k)+G_0(r,\omega)u_{12}(-k|-r|-p)]\\ &-\left[\frac{\epsilon(\omega)-1}{\epsilon(\omega)}\right]^3 G_0(q,\omega)G_0(r,\omega)u_{111}(p|q|r|k). \end{aligned} \tag{A3}$$

In addition, the following functions have been defined in Eq. (A3):

$$\begin{aligned} u_{12}(p|q|k)=&-iq^2[\alpha(p,\omega)\alpha(k,\omega)\Delta_-(p,\omega)\Delta_-(k,\omega)-pk\Delta_+(p,\omega)\Delta_+(k,\omega)]\\ &+pq\alpha(k,\omega)[\Delta_+(q,\omega)-1][qk-\alpha_0^2(q,\omega)]\Delta_+(q,\omega)\Delta_+(p,\omega)\Delta_+(k,\omega)\\ &+\alpha(p,\omega)\alpha(q,\omega)\left[\alpha_0(q,\omega)-\frac{\alpha(q,\omega)}{\epsilon(\omega)}\Delta_-(q,\omega)\right][qk-\alpha_0^2(k,\omega)]\Delta_-(q,\omega)\Delta_-(p,\omega)\Delta_+(k,\omega)\\ &+\left[\alpha_0(q,\omega)-\frac{\alpha(q,\omega)}{\epsilon(\omega)}\Delta_-(q,\omega)\right]\Delta_+(q,\omega)\\ &\quad\times\{\alpha(p,\omega)\alpha(k,\omega)[qk-\alpha_0^2(q,\omega)]\Delta_-(p,\omega)\Delta_-(k,\omega)+pq[\alpha^2(k,\omega)-qk]\Delta_+(p,\omega)\Delta_+(k,\omega)\}, \end{aligned} \tag{A4}$$

$$
\begin{aligned}
u_{111}(p|q|r|k)=&-pq^2r^2k[1-\Delta_+(q,\omega)][1-\Delta_+(r,\omega)]\Delta_+(p,\omega)\Delta_+(q,\omega)\Delta_+(r,\omega)\Delta_+(k,\omega)\\
&+\alpha(p,\omega)\alpha(k,\omega)\Delta_-(p,\omega)\Delta_-(k,\omega)\left[\alpha_0(q,\omega)-\frac{\alpha(q,\omega)}{\epsilon(\omega)}\Delta_-(q,\omega)\right]\\
&\times\left[\frac{\alpha(q,\omega)\alpha(r,\omega)}{\epsilon(\omega)}\Delta_-(q,\omega)\Delta_-(r,\omega)-qr\Delta_+(q,\omega)\Delta_+(r,\omega)\right]\left[\alpha_0(r,\omega)-\frac{\alpha(r,\omega)}{\epsilon(\omega)}\Delta_-(r,\omega)\right]\\
&+pqrk\frac{\alpha(q,\omega)\alpha(r,\omega)}{\epsilon(\omega)}\Delta_+(p,\omega)\Delta_-(q,\omega)\Delta_-(r,\omega)\Delta_+(k,\omega)\\
&+qr\Delta_+(q,\omega)\Delta_+(r,\omega)\left\{pq\alpha(k,\omega)[1-\Delta_+(q,\omega)]\left[\alpha_0(r,\omega)-\frac{\alpha(r,\omega)}{\epsilon(\omega)}\Delta_-(r,\omega)\right]\Delta_+(p,\omega)\Delta_-(k,\omega)\right.\\
&\left.+rk\alpha(p,\omega)[1-\Delta_+(r,\omega)]\left[\alpha_0(q,\omega)-\frac{\alpha(q,\omega)}{\epsilon(\omega)}\Delta_-(q,\omega)\right]\Delta_-(p,\omega)\Delta_+(k,\omega)\right\}\\
&-\left[\alpha_0(q,\omega)-\frac{\alpha(q,\omega)}{\epsilon(\omega)}\Delta_-(q,\omega)\right]\left[\alpha_0(r,\omega)-\frac{\alpha(r,\omega)}{\epsilon(\omega)}\Delta_-(r,\omega)\right]\\
&\times[pq\alpha(r,\omega)\alpha(k,\omega)\Delta_+(p,\omega)\Delta_+(q,\omega)\Delta_-(r,\omega)\Delta_-(k,\omega)\\
&+rk\alpha(p,\omega)\alpha(q,\omega)\Delta_-(p,\omega)\Delta_-(q,\omega)\Delta_+(r,\omega)\Delta_+(k,\omega)]\ . \qquad \text{(A5)}
\end{aligned}
$$

It should be noted that some lengthy algebraic manipulations have been performed in order to write $v_R^{(1)}$, $v_R^{(2)}$, $v_R^{(3)}$ in the forms presented above. In this way, upon recalling that $\alpha_0(q,\omega)$, $\alpha(q,\omega)$, $G_0(q,\omega)$, and $\Delta_\pm(q,\omega)$ are even functions of q, it is straightforward to show that the functions $v_R^{(1)}$, $v_R^{(2)}$, and $v_R^{(3)}$ satisfy the following properties, respectively:

$$v_R^{(1)}(p|k)=v_R^{(1)}(-k|-p)\ ,\quad v_R^{(2)}(p|q|k)=v_R^{(2)}(-k|-q|-p)\ ,\quad v_R^{(3)}(p|q|r|k)=v_R^{(3)}(-k|-r|-q|-p)\ .$$

These properties ensure the reciprocity of the three leading terms in the expansion of $V_R(p|k)$, Eqs. (4.37).

APPENDIX B

The contributions to $\langle \partial R_p/\partial\theta_s\rangle_{\rm incoh}$ through terms of fourth order in the surface profile function, Eq. (4.40), are given by

$$I_R^{(1-1)}(p|k)=\delta^2|v_R^{(1)}(p|k)|^2g(|p-k|)\ , \qquad \text{(B1)}$$

$$
\begin{aligned}
I_R^{(2-2)L}(p|k)=\delta^4\int_{-\infty}^{\infty}\frac{dq}{2\pi}g(|p-q|)g(|q-k|)\{&|v_R^{(2)}(p|q|k)|^2+2\,\mathrm{Re}[v^{(2)}(p|q|k)^*v_R^{(1)}(p|q)G_0(q,\omega)v_R^{(1)}(q|k)]\\
&+|v_R^{(1)}(p|q)G_0(q,\omega)v_R^{(1)}(q|k)|^2\}\ , \qquad \text{(B2)}
\end{aligned}
$$

$$
\begin{aligned}
I_R^{(2-2)C}(p|k)=\delta^4&\int_{-\infty}^{\infty}\frac{dq}{2\pi}g(|p-q|)g(|q-k|)\\
&\times\{v_R^{(2)}(p|k+p-q|k)^*v_R^{(2)}(p|q|k)+2\,\mathrm{Re}[v_R^{(2)}(p|k+p-q|k)^*v_R^{(1)}(p|q)G_0(q,\omega)v_R^{(1)}(q|k)]\\
&+\mathrm{Re}[v_R^{(1)}(p|p+k-q)^*G_0(p+k-q,\omega)^*v_R^{(1)}(p+k-q|k)^*v_R^{(1)}(p|q)G_0(q,\omega)v_R^{(1)}(q|k)]\}\ , \qquad \text{(B3)}
\end{aligned}
$$

$$
\begin{aligned}
I_R^{(1-3)}(p|k)=2\delta^4g(|p-k|)\,\mathrm{Re}\Bigg\{&v_R^{(1)}(p|k)^*\int_{-\infty}^{\infty}\frac{dq}{2\pi}\{g(|p-q|)[v_R^{(3)}(p|q|p|k)+v_R^{(2)}(p|q|p)G_0(p,\omega)v_R^{(1)}(p|k)\\
&+v_R^{(1)}(p|q)G_0(q,\omega)v_R^{(2)}(q|p|k)+v_R^{(1)}(p|q)G_0(q,\omega)v_R^{(1)}(q|p)G_0(p,\omega)v_R^{(1)}(p|k)\\
&+v_R^{(3)}(p|q|k-p+q|k)+v_R^{(2)}(p|q|k-p+q)G_0(k-p+q,\omega)v_R^{(1)}(k-p+q|k)\\
&+v_R^{(1)}(p|q)G_0(q,\omega)v_R^{(2)}(q|k-p+q|k)\\
&+v_R^{(1)}(p|q)G_0(q,\omega)v_R^{(1)}(q|k-p+q)G_0(k-p+q,\omega)v_R^{(1)}(k-p+q|k)]\\
&+g(|q-k|)[v_R^{(3)}(p|k|q|k)+v_R^{(2)}(p|k|q)G_0(q,\omega)v_R^{(1)}(q|k)\\
&+v_R^{(1)}(p|k)G_0(k,\omega)v_R^{(2)}(k|q|k)+v_R^{(1)}(p|k)G_0(k,\omega)v_R^{(1)}(k|q)G_0(q,\omega)v_R^{(1)}(q|k)]\}\Bigg\}\ , \qquad \text{(B4)}
\end{aligned}
$$

where the functions $v_R^{(1)}$, $v_R^{(2)}$, and $v_R^{(3)}$ are given in Appendix A.

*Present address: Instituto de Estructura de la Materia, CSIC, Serrano 121, 28006 Madrid, Spain.

[1]A. R. McGurn and A. A. Maradudin, Opt. Commun. **72**, 279 (1989).

[2]V. Celli, P. Tran, A. A. Maradudin, Jun Lu, T. Michel, and Zu-Han Gu, in *Laser Optics of Condensed Matter,* edited by E. Garmire, A. A. Maradudin, and K. K. Rebane (Plenum, New York, 1991), Vol. 2, pp. 315–324.

[3]Zu-Han Gu, R. S. Dummer, A. A. Maradudin, A. R. McGurn, and E. R. Méndez, Appl. Opt. **30**, 4094 (1991).

[4]Zu-Han Gu, A. A. Maradudin, E. R. Méndez, M. A. Ponce, and V. Ruiz-Cortés, Waves Random Media **1**, S75 (1991).

[5]V. D. Freilikher, M. Pustilnik, and I. Yurkevich, Phys. Lett. A **193**, 467 (1994).

[6]A. A. Maradudin and E. R. Méndez, Appl. Opt. **32**, 3335 (1993).

[7]J. A. Sánchez-Gil, A. A. Maradudin, Jun Q. Lu, V. D. Freilikher, M. Pustilnik, and I. Yurkevich, Phys. Rev. B **50**, 15 353 (1994).

[8]Lord Rayleigh, *The Theory of Sound Vol. II,* 2nd ed. (Macmillan, London, 1896), pp. 89 and 96.

[9]Lord Rayleigh, Proc. R. Soc. London Ser. A **79**, 399 (1907).

[10]F. Toigo, A. Marvin, V. Celli, and N. R. Hill, Phys. Rev. B **15**, 5618 (1977).

[11]G. C. Brown, V. Celli, M. Coopersmith, and M. Haller, Surf. Sci. **129**, 507 (1983).

[12]J. A. Ogilvy, *Theory of Wave Scattering from Random Rough Surfaces* (Hilger, Bristol, 1991), p. 39.

[13]J. M. Soto-Crespo, M. Nieto-Vesperinas, and A. T. Friberg, J. Opt. Soc. Am. A **7**, 1185 (1990).

[14]A. A. Maradudin, T. Michel, A. R. McGurn, and E. R. Méndez, Ann. Phys. (N.Y.) **203**, 155 (1990).

[15]J. A. Sánchez-Gil and A. A. Maradudin, Waves Random Media **4**, 499 (1994).

[16]A. A. Maradudin, E. R. Méndez, and T. Michel, in *Scattering in Volumes and Surfaces,* edited by M. Nieto-Vesperinas and J. C. Dainty (North-Holland, Amsterdam, 1990), pp. 157–174.

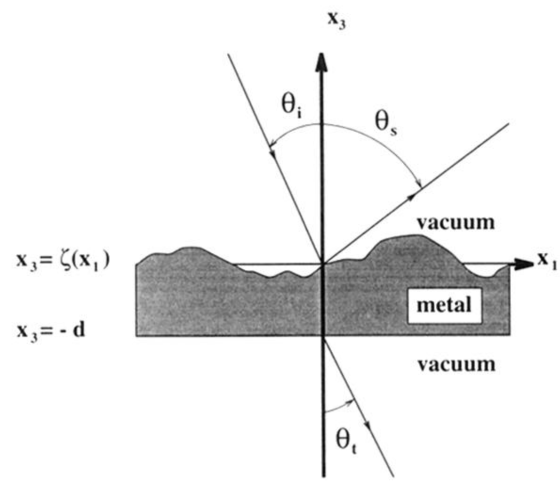

FIG. 2. The free-standing metal film studied in the present paper.